

CdI₂ nanoparticles with closed-cage (fullerene-like) structures

R. Popovitz-Biro, N. Sallacan and R. Tenne

Department of Materials and Interfaces, Weizmann Institute, Rehovot 76100, Israel

Received 5th March 2003, Accepted 23rd April 2003

First published as an Advance Article on the web 8th May 2003

It was shown previously that nanoparticles of layered compounds form closed-cage and nanotubular structures. These nanostructures received the generic name of inorganic fullerene-like (*IF*) materials. In particular nanoparticles of metal dihalides, like NiCl₂ and CdCl₂, were shown to form such closed-cage structures in the past. In the present report faceted *IF*-CdI₂ nanoparticles encapsulating a Cd core are reported. These nanoparticles were obtained using electron beam irradiation of the source powder of CdI₂. The faceted nanoparticles exhibit one of two morphologies: hexagonal or elongated rectangular characters. The nanoparticles can be considered as core (Cd)–shell (CdI₂) nanostructures. Consistent with previous observations, this study shows that the seamless structure of the *IF* materials can stabilize phases, which are otherwise unstable under the electron-beam irradiation. The growth mechanism of these nanostructures is briefly discussed.

Introduction

Graphite nanoparticles have been shown to undergo a spontaneous morphological transformation, which causes them to fold into fullerenes¹ and nanotubes.² The driving force for this process is known to be the abundance of dangling bonds at the periphery of the graphite slab. To induce the folding and closure, and thereby eliminate the dangling bonds, pentagons are introduced into the otherwise hexagonal network. The deviation from planarity of the sp² bonds induces substantial stress into the nanostructure, which is nevertheless more than compensated by the elimination of the dangling bonds. Therefore, the total energy of the nanostructure is minimized by formation of the closed cage.

Nanoparticles of inorganic compounds with layered structures have been also shown to be unstable in the planar form and spontaneously fold into hollow closed structures, including nanotubes—generically known as inorganic fullerene-like materials (*IF*). Nanotubes and fullerene-like structures have been obtained from various layered materials, such as MS₂^{3–6} (M = Mo, W; X = S, Se), NbS₂,⁷ InS,⁸ BN,⁹ metal halides like NiCl₂¹⁰ and CdCl₂,¹¹ oxides like, V₂O₅,¹² Ti₂O,¹³ H₂Ti₃O₇,¹⁴ and numerous other layered compounds.

CdI₂ forms a hexagonal lattice (*P*_{63mc} space group, 186), where each cadmium atom exists in an octahedral environment coordinated to 6 iodine atoms. The interlayer spacing (*c*-axis) is 0.68 nm (see Fig. 1). The shear between the layers does not involve large activation energy barriers, which may explain the abundance of different polytypes of this crystal. The most common polytypes are the 2H and 4H, with two and four repeat units arranged in hexagonal fashion. Closed polyhedra of CdCl₂ were obtained in the past by the reaction of CdCl₂·H₂O precursor with the electron beam during

transmission electron microscopy studies.¹¹ Here bulk cadmium chloride, which was exposed to the ambient, was found to always have one water molecule per formula, while the closed polyhedra of the same compound were found to be water free, and did not take up water even when they were exposed to the atmosphere. CdCl₂ polyhedra, which were obtained by e-beam irradiation were found to exhibit a very particular hexagonal morphology, which was previously found also in NiCl₂ polyhedra. In the present report CdI₂ powder is found to evaporate by the electron beam and recrystallize into closed polyhedra with hexagonal topology. Previously, closed shell MoS₂ nanoparticles with spherical morphology were obtained by electron-beam irradiation of MoS₂ powder.¹⁵ Pioneering work on the recrystallization of nested carbon fullerenes by e-beam irradiation of carbon soot was performed by Ugarte¹⁶ and Banhart.¹⁷ Similarly, crystallization of amorphous MoS₃ nanoparticles was obtained by inducing electrical pulses with the tip of a scanning probe microscope.¹⁸ The resulting nanoparticles assumed a core–shell structure, with a closed shell of MoS₂ and an amorphous MoS₃ core.

Experimental methods

CdI₂ powder was either synthesized from the elements or used as purchased. The powder was dry-placed onto a Cu grid. For the analysis of the samples, a transmission electron microscope (TEM), Philips model CM120 operating at 120 kV and equipped with an energy dispersive X-ray analyzer (EDS), EDAX model Pheonix, were used. A high resolution transmission electron microscope (HRTEM), Tecnai F-30 of FEI, equipped with an EELS spectrometer (Gatan), were also used for the analysis. X-Ray diffraction was done with a Rigaku Rotaflex RU200B equipped with a Cu anode.

Results and discussion

The XRD pattern of the precursor powder could be indexed according to the 2H polytype with a lattice spacing of 0.68 nm between the CdI₂ layers. The CdI₂ powder was found to be unstable under the electron beam, in the TEM and out-gassed during the analysis. Indeed, evaporation of the film and recrystallization of nanoparticles occurred during the TEM analysis. Fig. 2 displays a portion of the irradiated sample, before (a) and after (b) the irradiation. The irradiated zone

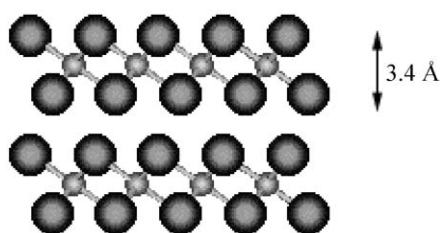


Fig. 1 Schematic representation of the 2H-CdI₂ lattice.

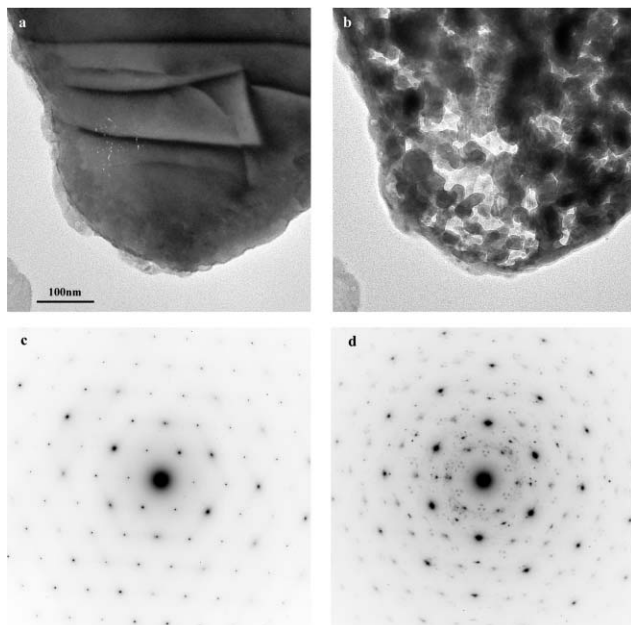


Fig. 2 TEM micrographs of a typical area of irradiated zone of CdI₂ grain, (a) before and (b) following the e-beam irradiation. The electron diffraction patterns of parts of the irradiated zone are shown in (c) before and (d) after irradiation.

appears like a “perforated” structure with numerous nanoparticles dispersed in the irradiated zone. Electron diffraction (ED) of the pristine material (c) exhibits a hexagonal pattern, which corresponds to the 2H-CdI₂ polytype. Surprisingly, the ED pattern of the irradiated zone (d), which was gathered from a relatively large area containing many nanoparticles, consists of isolated spots. This result can be understood by assuming that most of the ED signal is diffracted from areas which were not influenced by the e-beam. It could furthermore suggest that the recrystallized nanoparticles are aligned along several preferred orientations. EDS analysis of the sample showed that only cadmium and iodine were present in the sample and the Cd : I ratio varied from about 1 : 1.5 in the original sample to 2 : 1 in the irradiated nanoparticles. Thus iodine is lost

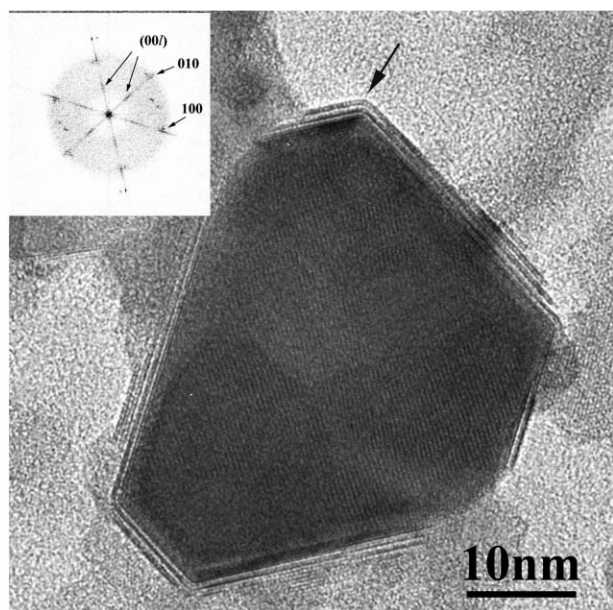


Fig. 3 TEM micrograph showing a typical CdI₂ nanoparticle with hexagonal projection formed under electron beam irradiation. Fringes of the CdI₂ layers encapsulating the non-hollow Cd containing core are clearly observed. The electron diffraction pattern of the crystallite is shown in the inset.

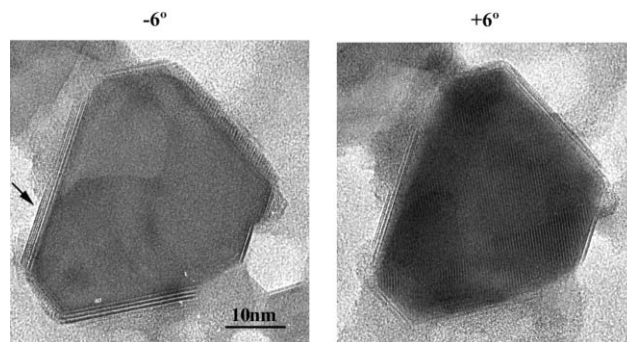


Fig. 4 TEM images of the same nanocrystal tilted through various angles (-6° and $+6^\circ$). The splitting of the fringes in the circumference of the nanoparticles into pairs of fringes (arrows) is clearly observed under certain tilt angles. These splits are believed to be the result of the scattering of the iodine layers within the CdI₂ lattice.

during the electron-beam irradiation of the film. The nanoparticles appeared only after some 10 min of irradiation time. Once obtained, the closed non-hollow polyhedra are found to be stable under the electron beam.

Further examination of the nanoparticles with TEM and ED shows that most of the polyhedra consist of a core-shell structure, in which a closed cage of CdI₂ enfold a denser core which consists of pure cadmium metal or a mixture of the metal and the original powder. This is not an uncommon situation and has been observed before, in *e.g.* electrically induced recrystallization of amorphous MoS₃ nanoparticles.¹⁸ Notwithstanding the relatively low melting (387°C) and boiling temperatures (796°C) of CdI₂, the present nanoparticles could have been formed by recrystallization from the vapor or the molten phase.

Fig. 3 shows a closed-cage CdI₂ nanoparticle with hexagonal projection akin to the CdCl₂ closed-cage structures reported earlier.¹¹ The core of the nanoparticle consists of a fringe pattern with spacing of about 0.4 nm, which extends over most of the crystal dimensions. This pattern is believed to be a Moiré pattern resulting from two superposed lattices of CdI₂ and Cd (see also Fig. 6 later). The Fourier transform pattern (inset) shows a hexagonal diffraction pattern of (*hk*0) and (00*l*), which is indicated by arrows, corresponding to the CdI₂ lattice. Furthermore, two weak spots with a *d*-spacing of about 0.4 nm and corresponding to the Moiré pattern are seen. The Moiré pattern disappears upon further tilting of the crystallite.

Fig. 4 shows the tilting of the nanoparticle which was displayed in Fig. 3 in various angles. This figure shows that the lattice fringes in the circumference of the hexagonal nanoparticle split into pairs of distinct fringes (arrows in Fig. 4 at -6° and $+6^\circ$ tilt angles). An exploded view of a part of the layers in

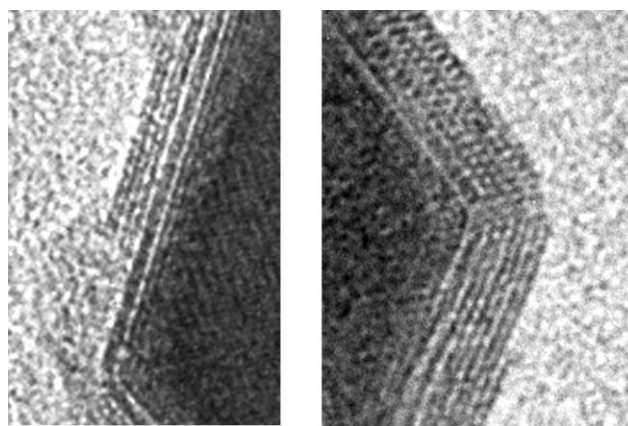


Fig. 5 Higher magnification of CdI₂ lattice fringes at the corners of two different polyhedra, clearly revealing the splitting of the molecular fringes into pair of lines.

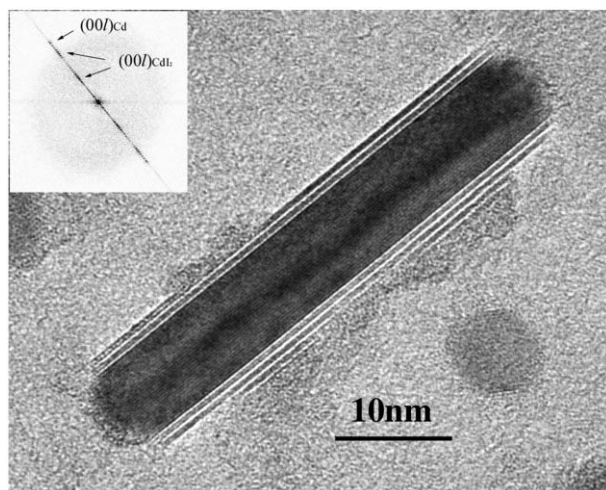


Fig. 6 TEM micrograph showing a typical elongated shape of a CdI_2 nanoparticle. Splitting of the fringes into pairs of fringes is also noticed.

the circumference of two corners of two different nanoparticles (Fig. 5) clearly reveals this phenomenon. This splitting is often observed upon tilting the nanoparticles in the TEM. The splitting of the fringes into pairs of fringes is attributed to the reflections of the iodine rows within the CdI_2 molecular shell (see Fig. 1). The separation between the iodine–iodine rows in the CdI_2 molecular layer (0.34 nm) coincides with the experimentally observed distance. These experiments indicate that this nanoparticle is indeed a closed and faceted polyhedron.

Fig. 6 shows another typical morphology of the CdI_2 nanoparticles observed in such samples. The elongated nanostructure is covered with 2–3 CdI_2 layers along its long axis. Each monolayer of CdI_2 appears as either a single or split pair of fringes, depending on the angle of the beam *vis-à-vis* the nanoparticle and the local contrast. The cores of the elongated nanoparticles exhibit fringes of much smaller d -spacing (0.28 nm), which coincides with the (002) distance of elemental cadmium. The Fourier transform of this image (inset of Fig. 6) consists of a series of reflections, which coincide with the (00 l) hexagonal lattices of Cd (0.28 nm) and CdI_2 (0.68 nm), respectively. The tips of the elongated nanostructure adopt a conical shape and in some cases a few fringes of the encapsulating CdI_2 can be resolved at these two edges. It is assumed that the elongated nanostructure is in fact a side-on view (90° tilt) of the same kind of hexagonal nanoparticles shown in Figs. 2 and 3. Fig. 7 shows a schematic presentation of the polyhedral nanoparticle viewed by the TEM along two main axes, perpendicular to each other. The projected image of the nanoparticle produces a hexagonal structure along one axis and a rectangular structure along the perpendicular axis. However, a tilt of 90° , which would allow one to inspect the same nanoparticle along the two main axes, could not be performed with the present TEM setup. Although it is very difficult to tilt the sample so as to get an image of the fringes at the edges, they were nevertheless observed in HRTEM analysis of two polyhedra (not shown).

The growth mechanism of these polyhedral nanoparticles is currently not fully understood. The high melting point of elemental cadmium entails that it probably can not be evaporated by the electron beam. On the other hand, CdI_2 can be possibly evaporated by the electron beam. After evaporation, the volatile cadmium iodide clusters lose some or all of their iodine content. The remaining Cd nanoparticles redeposit on the substrate and become nucleation sites for the reaction with the free iodine in the gas atmosphere of the TEM column. Once the first few closed CdI_2 layers have been formed around the Cd core, the reaction ceases and

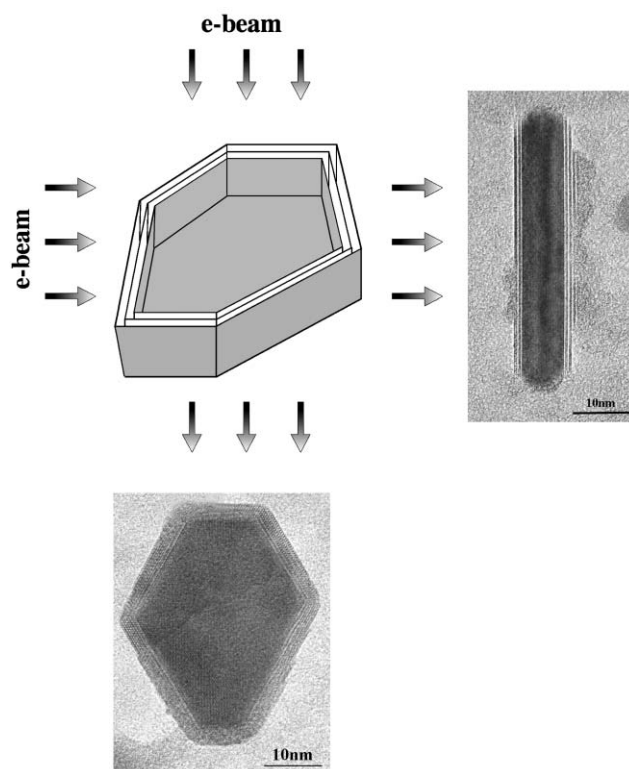


Fig. 7 A schematic drawing showing the polyhedral nanoparticle viewed by TEM along the two main axes: one leading to a hexagonal shaped structure, while the other produces a rectangular silhouette. Included also are the respective TEM images.

irradiation-resistant nanoparticles are formed. The diffusivity of the large iodine atoms through the first few layers of CdI_2 , which encapsulate the Cd core, is slow. Therefore the reaction ceases after a few closed CdI_2 layers have been formed encapsulating the Cd core, which therefore remains intact. This is to be contrasted with the synthesis of fullerene-like WS_2 nanoparticles from the respective oxide nanoparticles, where sulfur diffuses through the outer closed WS_2 layers and gradually converts the entire oxide core into sulfide.⁵

The most important issue, which remains unresolved, is the molecular structure of the edges and the rhombus corners. Polyhedra with hexagonal cross-section exhibiting oblique angles of 120° are typically observed in nanoparticles of layered metal halides, like NiCl_2 ,¹⁰ CdCl_2 ¹¹ and the present compound. The bending modulus of these highly ionic compounds, is very high, in comparison to *e.g.* metal dichalcogenide compounds. Therefore, they are not likely to form evenly bent nanostructures, like their MS_2 ($\text{M} = \text{Mo}, \text{W}$) predecessors. The energetically favorable topology in this case consists of a faceted structure with low angle grain boundaries. Combining high resolution transmission electron microscopy and first principle calculations, one may hope to shed light on the structure of these nanoparticles.

Acknowledgements

This work was carried out with the support of the Israel Science Foundation; the Minerva Foundation (Munich) and the G.M.J. Schmidt Minerva Center.

References

- 1 H. W. Kroto, J. R. Heath, S. C. O'Brien, R. F. Curl and R. E. Smalley, *Nature*, 1985, **318**, 162.
- 2 S. Iijima, *Nature*, 1991, **354**, 56.
- 3 R. Tenne, L. Margulis, M. Genut and G. Hodes, *Nature*, 1992, **360**, 444.

- 4 L. Margulis, G. Salitra, R. Tenne and M. Talianker, *Nature*, 1993, **365**, 113.
- 5 Y. Feldman, E. Wasserman, D. A. Srolovitz and R. Tenne, *Science*, 1995, **267**, 222.
- 6 M. Hershfinkel, L. Gheber, V. Volterra, J. L. Hutchinson, L. Margulis and R. Tenne, *J. Am. Chem. Soc.*, 1994, **116**, 1914.
- 7 (a) M. Nath and C. N. R. Rao, *J. Am. Chem. Soc.*, 2001, **123**, 4841; (b) M. Remskar, A. Marzel, A. Jesih and F. Lévy, *Adv. Mater.*, 2002, **14**, 680; (c) Y. Q. Zhu, W. K. Hsu, H. W. Kroto and D. R. M. Walton, *J. Phys. Chem. B*, 2002, **106**, 7623.
- 8 J. A. Hollingsworth, D. M. Poojary, A. Clearfield and W. E. Buhro, *J. Am. Chem. Soc.*, 2000, **122**, 3562.
- 9 N. G. Chopra, J. Luyken, K. Cherry, V. H. Crespi, M. L. Cohen, S. G. Louie and A. Zettl, *Science*, 1995, **269**, 966.
- 10 (a) Y. Rosenfeld-Hacohen, E. Grunbaum, R. Tenne, J. Sloan and J. L. Hutchinson, *Nature*, 1998, **395**, 336; (b) Y. Rosenfeld-Hacohen, R. Popovitz-Biro, E. Grunbaum, Y. Prior and R. Tenne, *Adv. Mater.*, 2002, **14**, 1075.
- 11 R. Popovitz-Biro, A. Twersky, Y. Rosenfeld Hacohen and R. Tenne, *Isr. J. Chem.*, 2001, **41**, 7.
- 12 M. E. Spahr, P. Bitterli and R. Nesper, *Angew. Chem., Int. Ed.*, 1998, **37**, 1263.
- 13 S. Avivi, Y. Mastai and A. Gedanken, *J. Am. Chem. Soc.*, 2000, **122**, 4331.
- 14 G. H. Du, Q. Chen, R. C. Che, Z. Y. Yuan and L.-M. Peng, *Appl. Phys. Lett.*, 2001, **79**, 3702.
- 15 M. Jose-Yacamán, H. Lopez, P. Santiago, D. H. Galvan, I. L. Garzon and A. Reyes, *Appl. Phys. Lett.*, 1996, **69**, 1065.
- 16 D. Ugarte, *Nature*, 1992, **359**, 707.
- 17 F. Banhart, *Nature*, 1996, **382**, 433.
- 18 M. Homyonfer, B. Alperson, Y. Rosenberg, L. Sapir, S. R. Cohen, G. Hodes and R. Tenne, *J. Am. Chem. Soc.*, 1997, **119**, 2693.